Magnetoluminescence

Jung-Tsung Li

Department of Physics, University of California, San Diego, CA 92093, USA

(Dated: March 12, 2020)

Abstract

Magnetoluminescence refers to a rapid conversion of (electro-)*magnetic* energy into the emission of non-thermal high-energy particles and γ-rays through dissipation in a short amount of time. Flares rapidly occur, and a large region becomes *luminous*.

Active galactic nuclei, pulsar wind nebulae, gamma ray burst, blazar, and magnetar generate strong magnetic-dominated winds which the electromagnetic energy flux is much higher than the plasma energy flux over a large region. Observations of γ-rays and high-energy particles from these sources show a variable broad non-thermal spectrum that is emitted by the accelerated electrons and positrons. Occasionally, a portion of these particles is rapidly accelerated to their radiation reaction limits (i.e., $\mathbf{E} \sim \mathbf{B}$) in a light-crossing timescale and produces a flare. This process and the phenomena is referred as *magnetoluminescence*. In these extreme environments, magnetic reconnection of the magnetic "ropes" is inevitable and it explains the origin of high energy particles. However, the characteristic scaling speed is c divided by a logarithmic change of volume, which is ~ 10, and it wasn't clear if the the process can dissipate magnetic energy in a large volume in a light-crossing time. On the other hand, it is possible that these magnetic ropes can untangle themselves in a light-crossing timescale without changing topology. This process is generally faster than the reconnection. It has been proposed that the dissipation can happen during the distangling by the small-scale electric shear stress–the wandering fields at the boundary of the magnetic flux tubes–and the dissipated magnetic energy can cause the rapid variability of the energetic particles and γ-ray emissions. Clearly, the underlying microphysics of the relativistic MHD and the kinetic models are necessary to understanding the variability of flares and the proton accelerations.

I. INTRODUCTION

The recent observation of dramatic γ-ray flare activities and their rapid variability has challenged the conventional particle acceleration mechanisms. It has been reported that the flares occurring in the Crab Nebula emit strong non-thermal γ-ray spectrum in the energy range ~ 100 MeV to 1 GeV in about ~ 1 event per year [1, 2]. The biggest flares have the timescale variation as short as few hours [3], with the peak luminosity $\sim 10^{36}$ erg/s and the total radiation energy $\sim 10^{40}$ erg [4]. This rapid variability events are also reported in many other extreme astrophysical sources. For example, several active galactic nuclei (AGN) are observed to flare in the GeV to TeV band with the time variation in only few minutes [5]. The gamma ray burst events also flares γ-ray on timescale as short as ~ 10 ms. These rapid variability of flares indicates that the energy conversion are not steady but rather intermittent, and, at the same time, the emission process can occur in an extented volume in their light crossing timescales.

The rapid variation of the flares are likely linked to the electromagnetic-dominated, relativistic jets/winds from the center of the sources, e.g., black holes and spinning neutron stars. The magnetic energy of these outflows are dissipated at distances away from the source, and electrons and positrons are able to be accelerated to their radiation reaction limits and bremss off a burst of γ-rays in the light crossing timescales. The problem is how this can happen so rapidly.

A. Why we study this?

It has been known that the magnetic reconnection can convert magnetic energy into particle kinetic energy by changing the magnetic field topology. The Sweet-Parker model, which assumes that the reconnection happen in a plane, is extremely slow as the reconnection rate $r_{\rm rec} \equiv v_{\rm in}/v_{\rm out} \sim 1/\sqrt{R_{\rm m}}$, where $R_{\rm m} \sim LV_A/\eta$ is the magnetic Reynold's number and L, V_A and η are the scale of the system, the Alfven speed, and the magnetic diffusivity, respectively. On the other hand, the fast reconnection may occur in the Petschek model because it assumes the reconnection occurs in a X-point instead of a plane. The reconnection rate in Petschek model is $r_{\rm rec} \sim 1/\ln(R_{\rm m})$ and is many orders of magnitude larger than the rate in Sweet-Parker model. It has been shown that the relativistic Petschek model together with the kinetic effects (e.g., tearing instability) can produce the anomalous resistivity which stabilizes the shock configuration at X-points and also enhances the reconnection rate to $r_{\rm rec} \lesssim 0.1$ [6, 7]. However, fact that the all the flux have to go through a tiny region at the X-point suggests that the relativistic reconnection is still slow and it wasn't clear if a large volume of magnetic energy can really dissipate rapid enough to explain the high-energy particles and the flare of γ-rays.

In this paper, I will look into a fairly recent idea proposed by Blandford's group regarding the Taylor relaxation of a force-free equilibria driven by the outflow [4, 8]. It was found that the short wavelength magnetostatic equilibria of a strongly magnetized plasma is unstable to the ideal MHD modes, and it leads to the formation of current sheets where the magnetic energy dissipation and the particle acceleration occurs. This magnetic instability saturates through turbulent relaxation and eventually the system relaxes to the lowest order state with the conservation of magnetic

helicity. The dissipation of magnetic energy from this mechanism can happen in just one light crossing time which is an encouraging explanation for the rapid variability of the flares.

The name *magnetoluminescence* is invented by Roger Blandford [9]. It refers to a rapid conversion of magnetic energy over a large volume into the non-thermal high-energy particles and γ-rays. If dissipation of magnetic energy is rapid and efficient, then the magnetic energy support may suddenly drop a lot and not be able to hold up the external pressure which may lead to implosion and further dissipation. The process is analogous to *sonoluminescence* in which the sound wave produces a gaseous cavity in the water and leads to implosion and the short burst of X-ray and ultraviolets.

In the following, I will explain the magnetic instability in the relativistic MHD description in Sec. II and the kinetic description in Sec. III. An analogy of magnetic hairy ropes will be given in Sec. IV. And lastly the discussion is given in Sec. V.

II. RELATIVISTIC MHD DESCRIPTION

Taylor conjecture states that the global magnetic helicity in a closed, magnetically dominated plasma is conserved as the system minimizes its magnetic energy to the lowest energy state. That is, the action is minimized and the magnetic helicity serves as a Lagrangian multiplier,

$$\delta\left[\int_{\rm V}\frac{|\mathbf{B}|^2}{8\pi}d^3x+\lambda\int_{\rm V}\mathbf{A}\cdot\mathbf{B}\,d^3x\right]=0, \tag{1}$$

where magnetic helicity is given as

$$H_{\rm m}=\int_{\rm V}\mathbf{A}\cdot\mathbf{B}\,d^3x. \tag{2}$$

This process of minimization is caused by the turbulent relaxation, and the magnetic energy is released as the system is relaxing to the lowest order state. The end state of the magnetic configuration is homogenized and force-free, that is, $\nabla\times\mathbf{B}=\alpha\mathbf{B}$, where α is a constant. This profile is called Taylor state. The Taylor hypothesis suggests a selective decay: the system manages to cascade its magnetic energy at small scales while inverse-cascades the magnetic helicity and piles them at the largest scale so that the global magnetic helicity remains constant as the turbulent relaxation occurs.

Therefore, we would want to know whether or not a local region in the outflow with a tangled magnetic field topology can undergo turbulent relaxation and how fast it can happen. Reference [8] considers a force-free magnetostatic equilibria with $\nabla\times\mathbf{B}=\alpha\mathbf{B}$ and simulate its evolution with a relativistic MHD code. The simulation is done under a 3D periodic Cartesian box and the configuration has a topology of magnetic fluxes packed together. In particular, the solution of the equilibrium magnetic field is chosen as

$$\mathbf{B}^{\rm E}=(B_3\cos\alpha z-B_2\sin\alpha y)\,\hat{\mathbf{x}}+(B_1\cos\alpha x-B_3\sin\alpha z)\,\hat{\mathbf{y}}+(B_2\cos\alpha y-B_1\sin\alpha x)\,\hat{\mathbf{z}}, \tag{3}$$

where B_1, B_2, and B_3 are the three free parameters. The corresponding velocity field is given by $\mathbf{v}=\mathbf{E}\times\mathbf{B}^{\rm E}/|\mathbf{B}^{\rm E}|^2$.

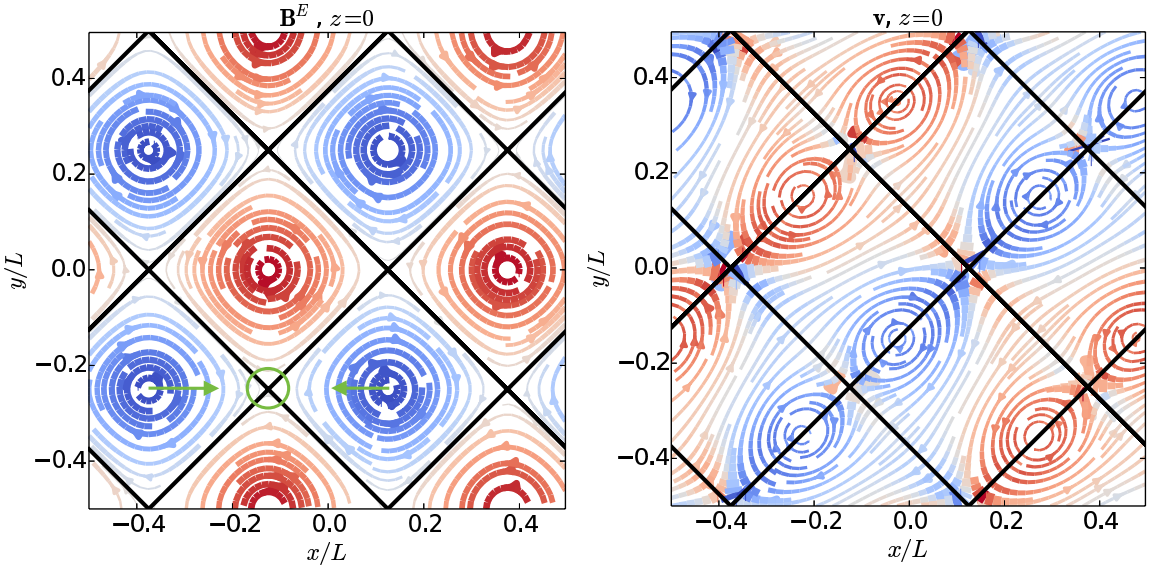

FIG. 1. The streamline of magnetic fields (left) and the corresponding velocity fields (right) of a force-free equilibria with $\alpha = 2$. The equilibrium solution is chosen as $(B_1, B_2, B_3) = (1, 1, 0)$. The red (blue) indicates a perpendicular vector component with out of the page (into the page) direction. The green circle is a location of the reconnection of the bottom two blue vortices in the left plot. (The figure is taken from Ref. [8].)

It is found that the unstable mode of Eq. 3 occurs only when $|\alpha| > 1$. So as an illustration to show the nature of magnetic instability, a simple solution to instability is chosen: $\alpha = 2$ and $(B_1, B_2, B_3) = (1, 1, 0)$. The structure of $(B_1, B_2, B_3) = (1, 1, 0)$ is a helical field and current lines spiraling along the z direction. Its magnetic field line configuration and the corresponding velocity field line is shown in Fig. 1. The velocity field from the right panel shows that the bottom two blue "vortices" on the left panel are merging to each other which results in a reconnection occurring at the X-point (circled in green). It is an indication that the magnetic instability and relaxation is a series of magnetic flux tube merging and shearing.

Figure 2 shows the magnetic energy ($U_{\rm B}$) and kinetic energy ($U_{\rm E}$) evolutions and the comparisons of various magnetization parameters. The magnetization parameters is defined as $\sigma \equiv \langle B^2/4\pi\rho h\rangle$ where ρh is the fluid enthalpy. The initial magnetic configuration is chosen with the $\alpha^2 = 11$ equilibrium. The two horizontal dashed lines in the top panel correspond to the magnetic energy of $\alpha^2 = 3$ (the intermediate state) and $\alpha^2 = 1$ (the ground state). It is shown that different values of σ still evolve to the same intermediate and ground states. The only difference is the Alfven crossing time: a larger σ equilibria relaxes faster to its ground state.

The feature that different values of σ equilibria all evolve to the same intermediate state ($\alpha^2 = 3$) and ground ($\alpha^2 = 1$) state suggests that the turbulent relaxation conserves its magnetic helicity. This can be seen from the fact that the force-free solution, $\nabla \times \mathbf{B} = \alpha\mathbf{B}$, or equivalently, $\mathbf{B} = \alpha\mathbf{A}$, have the magnetic helicity $H_{\rm m} \sim U_{\rm B}/\alpha$. It can be seen in Fig. 2 that the ratio of $U_{\rm B}$ to α stays the same for all values of σ as the equilibria evolves. That is, the magnetic energy is dissipated at the small wavelength states (seen in Fig. 1) while the magnetic helicity is piled up at the largest possible

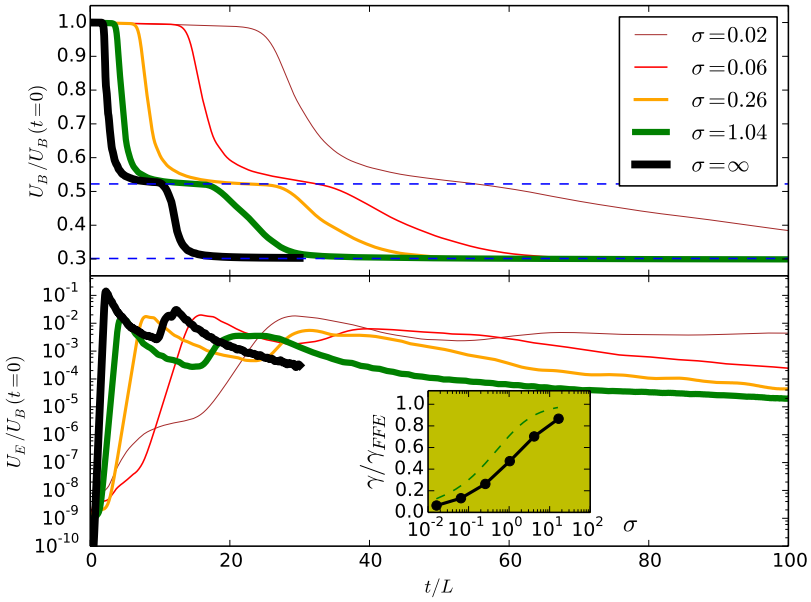

FIG. 2. The evolution of the $\alpha^2 = 11$ magnetic configuration with various magnetization parameter σ. (**top panel**) In all cases of σ, the equilibria evolves to the same intermediate ($\alpha^2 = 3$) and ground state ($\alpha^2 = 1$). The magnetic helicity $H_{\rm m} \sim U_{\rm B}/\alpha$ remains constant as the system relaxes. (**bottom panel**) The kinetic energy $U_{\rm E}$ undergoes exponential growth in the early stage of instability. In the case which $\sigma = \infty$, we see $|\mathbf{E}|$ grows to the level that is comparable to $|\mathbf{B}|$ within just one dynamical time. (The figure is taken from Ref. [8].)

wavelength state which conserves the global magnetic helicity (seen in Fig. 2). The magnetic energy difference between initial and final states then serves as a free energy for this turbulent relaxation process.

The bottom panel of Fig. 2 shows that a relativistic plasma with a high σ can lead to an exponentially growing instability in which case $|\mathbf{E}|$ rises to the level that is comparable to $|\mathbf{B}|$ within just one dynamical timescale (i.e., a light crossing time to a relativistic plasma outflow). If this phenomena does occur in Crab Nebula or quasars, then it can be a strong candidate mechanism for the extreme particle acceleration and the γ-ray flares.

III. KINETIC DESCRIPTION

A similar magnetic configuration has also been studied in the kinetic description. Reference [4] has investigated the evolution of particle distribution function in phase space and the stability on kinetic simulation with the code Particle in cell (PIC) Zeltron. Their goal is to understand the underlying physics of electromagnetic dissipation and the emission spectrum from the accelerated particles. And it was found that more interesting physics at the evolution stage is obtained from the PIC simulation compared to the relativistic MHD simulation, in particular plasmoid generation at the edge of the current sheet and the beaming of accelerated particles. While there are many fruitful physics from the PIC simulation, I will not discuss all of them. Instead, in this section, I

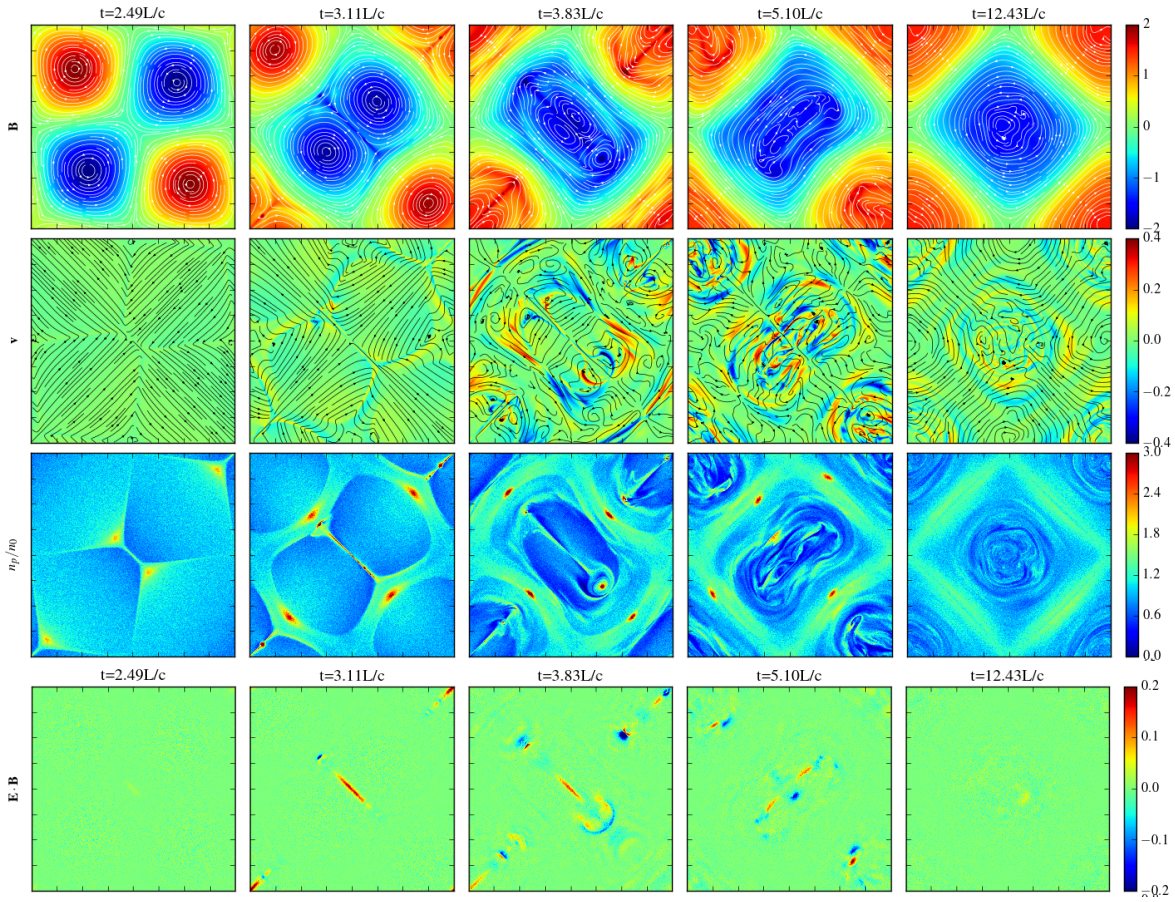

FIG. 3. The snapshots of the PIC simulation. The streamline indicates the in-plane field direction and the color indicates the vector component in $\hat{z}$ direction. From the top to bottom panels: magnetic field lines, velocity fields, proton number density, and $\mathbf{E}\cdot\mathbf{B}$. At the time of current sheet formation (second column), $\mathbf{E}\cdot\mathbf{B}$ reaches maximum (4th row), and the number density of particles at the current sheet is high due to shock formation. At the edges of the current sheet, the number density is particularly high due to the fact that the blobs ejected out from the current sheet experiences a Lorentz force and the particles decelerate. (The figure is taken from Ref. [4].)

will focus on the kinetic effect to the conservation of global magnetic helicity and the generation of $\mathbf{E}$ at the current sheets.

The initial condition of the magnetic field is given as

$$\mathbf{B}^{\mathrm{E}} = \sqrt{2}B_0\left(\sin kx\cos ky, -\cos kx\sin ky, -\sin kx\sin ky\right), \tag{4}$$

which satisfies $\nabla\times\mathbf{B} = -\sqrt{2}k\mathbf{B}$. In Fig. 3, the PIC simulation also shows a very similar features as the result from MHD simulation. Initially, the two blue magnetic tubes merge to each other and form a current sheet at the interface and it happens in as fast as one dynamical timescale. The particle number density is higher in the current sheet than in the ambient plasma. The number density peaks at the edge of the current sheet because the ejecting blobs undergo Lorentz force from ambient magnetic field and thus decelerate. In about 10 dynamical times, the two vortices can merge and relax to the ground state. The current sheet is actually very short-lived in the

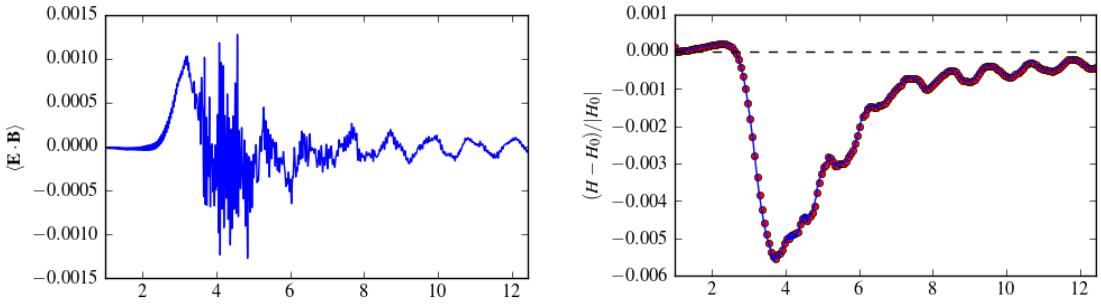

FIG. 4. The left panel is the time evolution of $\langle \mathbf{E} \cdot \mathbf{B} \rangle$. The right panel is the change of magnetic helicity. In both plots, the horizontal axis is t/L where L represents one wavelength of the magnetic tube. In the right panel, the blue solid line is the theoretical values of the rate change magnetic helicity, $dH_{\rm m}/dt = -2 \int \mathbf{E} \cdot \mathbf{B}\, d^3x$, and the red dots are the simulation result. (The figure is taken from Ref. [4].)

evolution, lasting no more than 1 dynamical time.

The bottom row of Fig. 3 shows the strength of $\mathbf{E} \cdot \mathbf{B}$. It is shown that at the stage of current sheet formation, the $\mathbf{E} \cdot \mathbf{B}$ reaches maximal which is expect since the magnetic energy dissipation happens at the location where the reconnection happens. Figure 4 shows the volume-averaged evolution of $\langle \mathbf{E} \cdot \mathbf{B} \rangle$ and the change of magnetic helicity. The rate change of helicity is given as

$$\frac{dH_{\rm m}}{dt} = -2 \int \mathbf{E} \cdot \mathbf{B}\, d^3x. \tag{5}$$

So the fact that the magnetic helicity remains constant (shown in the right panel of Fig. 4) indicates that the volume integral of $\mathbf{E} \cdot \mathbf{B}$ remains small even though (1) locally $\mathbf{E} \cdot \mathbf{B}$ can reach high values and (2) a large fraction of magnetic energy is lost during the reconnection process.

IV. ANALOGY

The magnetic fields on the xy plane shown in Fig. 1 carry the charge currents in the z direction. One can imagine that the current twist itself and thus twists the magnetic fields and form a "hairy" magnetic rope [10]. The "hair" would be the wandering magnetic fields at the surface of the rope. The ropes may tangle themselves in ways similar to fluid-type instabilities (e.g., Rayleigh-Taylor instability). If they are tangled into a hitch in which the topology is not changed, as shown in Fig. 5, then they can also be untangled. The distangling can happen within light crossing timescale which might be an explanation of the rapid variability of the γ-ray flares.

The dissipation comes from the "friction" between the ropes. In the case of MHD ropes, the friction is the electric shear stress between the two magnetic ropes slipping through each other. That is, the nonzero $\mathbf{E} \cdot \mathbf{B}$ comes from the slicing of two section of the ropes as the rope is trying to untangle itself. The same analogy also says that the small scale magnetic ropes (or the "hairs") are broken due to the electric shear stress (or the "friction"). However, the global structure of the rope remains intact, so the total magnetic helicity is conserved globally.

That is to say, we want to consider the alternative of global magnetic reconnection from swapping and reconnecting global magnetic field tubes because reconnection changes topology which is too

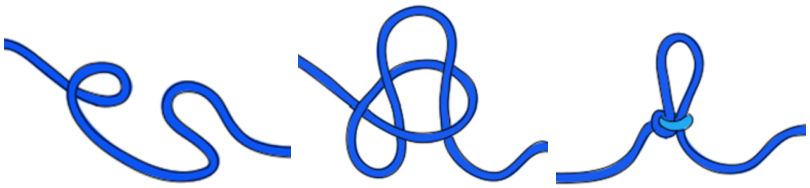

FIG. 5. The topology of the hitch. The blue rope is analogous to global magnetic tube and the friction between the ropes is analogous the the electromagnetic shear stress that makes $\mathbf{E} \cdot \mathbf{B} \neq 0$.

slow. Without the major change of topology, it is possible that the distangling can happen in one light crossing time and still dissipate a significant fraction of magnetic energy.

V. DISCUSSION

The simulations in MHD and kinetic descriptions both start with two magnetic flux tubes that spiral helically as the initial configuration. That is, the initial force-free solution is already unstable and there is free magnetic energy stored in the structure. But it is not clear if the strong magnetic dominated winds can really make that configuration and later untangles themselves. And currently there is very little understanding from both observation and simulation as of how nature form such ties in the winds.

On the other hand, the kinetic effects from PIC simulations provides many detailed effects that were not mentioned in here, such as the power spectral density of accelerated particles and γ-rays, the beaming effects, the polarization degrees, etc. They can be the predictions or signatures of the magnetic instability mechanism once more observations of the flaring activities from Event Horizon Telescope, the LSST and other telescopes are completed.

[1] A. Abdo, M. Ackermann, M. Ajello, A. Allafort, L. Baldini, J. Ballet, G. Barbiellini, D. Bastieri, K. Bechtol, R. Bellazzini, *et al.*, Science **331**, 739 (2011).

[2] R. Bühler and R. Blandford, Reports on Progress in Physics **77**, 066901 (2014).

[3] R. Bühler, J. Scargle, R. Blandford, L. Baldini, M. Baring, A. Belfiore, E. Charles, J. Chiang, F. D'ammando, C. Dermer, *et al.*, Astrophys. J. **749**, 26 (2012).

[4] Y. Yuan, K. Nalewajko, J. Zrake, W. E. East, and R. D. Blandford, Astrophys. J. **828**.

[5] J. Albert *et al.*, Astrophys. J. **669**, 862 (2007), arXiv:astro-ph/0702008 [astro-ph].

[6] J. Birn and M. Hesse, Journal of Geophysical Research: Space Physics **106**, 3737 (2001).

[7] B. Cerutti, G. R. Werner, D. A. Uzdensky, and M. C. Begelman, Astrophys. J. **770**, 147 (2013), arXiv:1302.6247 [astro-ph.HE].

[8] W. E. East, J. Zrake, Y. Yuan, and R. D. Blandford, Phys. Rev. Lett. **115**, 095002 (2015), arXiv:1503.04793 [astro-ph.HE].

[9] R. D. Blandford, *Extreme Astrophysics* (March 29, 2019), https://youtu.be/4ULTB_sCeuE?t=2620.

[10] R. Blandford, Y. Yuan, M. Hoshino, and L. Sironi, Space Sci. Rev. **207**, 291 (2017), arXiv:1705.02021 [astro-ph.HE].